

# A New Method for Dynamic Brain Connectivity Analysis Based on Tensor Decomposition in Tinnitus Using High-density Electroencephalogram in Source Domain

## Abstract

**Background:** Functional connectivity (FC), defined as the statistical reliance among different brain regions, has been an effective tool for studying cognitive brain functions. The majority of existing FC-based research has relied on the premise that networks are temporally stationary. However, there exist few research that support nonstationarity of FC which can be due to cognitive functioning. However, still there is a gap in tracking the dynamics of FC to gain a deeper understanding of how brain networks form and adapt in response to therapeutic interventions by identifying the change points that signify substantial shifts in network connectivity across the participants. **Methods:** The proposed approach in this study is based on tensor representation of FC networks of the source signals of electroencephalogram (EEG) activities yielding a multi-mode tensor. Then analysis of variance has been used to investigate changing points in connectivity of brain activity in sources domain in different conditions of tasks, frequency bands, and among subjects in time. High-density EEG signals (256 channels) were acquired from 30 tinnitus patients under visual (positive emotion induction) and transcranial direct current stimulation (tDCS) stimuli. **Results:** The proposed method of this study could effectively identify the significant brain connectivity change points, indicating enhanced effectiveness in capturing connectivity shifts comparing to conventional methods. Findings in tinnitus patients suggest that visual stimulation alone may not significantly alter brain connectivity networks. **Conclusion:** Based on the results, a combination of visual stimulation with simultaneous High-Definition tDCS is recommended, potentially informing optimal intervention strategies to enhance tinnitus treatment effectiveness.

**Keywords:** *Electroencephalogram, functional connectivity, tensor decomposition, tinnitus*

Submitted: 28-Nov-2024

Revised: 28-Dec-2024

Accepted: 22-Jan-2025

Published: 06-Aug-2025

## Introduction

Functional connectivity (FC) is described as the statistical dependence of distinct regions or the flow of information among them.<sup>[1,2]</sup> The majority of extant FC studies assume that networks are temporally stationary. Recent empirical research show that FC is dynamic due to cognitive functioning.<sup>[1]</sup> The trend in connectivity analysis is increasingly moving toward identifying dynamic changes. By detecting these critical transitions, researchers can gain a deeper understanding of how brain networks form, dissolve, and reorganize in response to cognitive demands in time or frequency.

Complementary approaches for tracking dynamic FC (dFC) have been developed

This is an open access journal, and articles are distributed under the terms of the Creative Commons Attribution-NonCommercial-ShareAlike 4.0 License, which allows others to remix, tweak, and build upon the work non-commercially, as long as appropriate credit is given and the new creations are licensed under the identical terms.

For reprints contact: WKHLRPMedknow\_reprints@wolterskluwer.com

based on clustering of FC networks (FCNs) and component analysis base approaches, respectively. One approach involves clustering FCNs across time and subjects, based on the assumption that the network occupies a distinct state at each time point, with these states varying over time.<sup>[3-5]</sup> For instance, Allen *et al.*<sup>[3]</sup> introduced a data-driven approach utilizing k-means clustering to identify “FC-states” from resting-state Functional magnetic resonance imaging (fMRI) data. Similar clustering-based methods for identifying FC states have been employed in electroencephalogram (EEG) studies.<sup>[4,5]</sup>

Leonardi *et al.*<sup>[6]</sup> proposed principal component analysis (PCA)-based method designed to capture key fluctuations in whole-brain FC. In this approach, network

**How to cite this article:** Bahman M, Sajadi SS, Toostani IG, MakkiAbadi B. A new method for dynamic brain connectivity analysis based on tensor decomposition in tinnitus using high-density electroencephalogram in source domain. *J Med Signals Sens* 2025;15:23.

Moein Bahman<sup>1</sup>,  
Seyed Saman  
Sajadi<sup>1</sup>,  
Iman Ghodrati  
Toostani<sup>1</sup>,  
Bahador  
MakkiAbadi<sup>1,2</sup>

<sup>1</sup>Department of Medical Physics and Biomedical Engineering, School of Medicine, Tehran University of Medical Sciences, Tehran, Iran, <sup>2</sup>Research Centre for Biomedical Technologies and Robotics, Tehran University of Medical Sciences, Tehran, Iran

## Address for correspondence:

Dr. Bahador MakkiAbadi,  
Department of Biomedical  
Engineering and Medical  
Physics, School of Medicine,  
Tehran University of Medical  
Sciences, Poursina Street,  
Tehran, Iran.  
E-mail: makkiabadib@gmail.  
com

## Access this article online

Website: [www.jmssjournal.net](http://www.jmssjournal.net)

DOI: 10.4103/jmss.jmss\_75\_24

## Quick Response Code:



states are represented by eigen connectivities that explain the largest variance within a series of dFC networks across time and subjects. These selected eigen connectivities serve as foundational elements of dFC, with subject-specific, time-dependent weights calculated through orthogonal projection to indicate each eigen connectivity's influence.<sup>[7,8]</sup>

It is also important to investigate the time and regions where connectivity indeed changes due to stimulation across conditions as well as dynamic changes. In practice, latent components, such as between brain sources, are complex and rarely statistically independent. Hence, there would be a need to decompose these components to identify the changing states in time or space. Linear data models, such as PCA<sup>[9]</sup> and independent component analysis (ICA)<sup>[10]</sup> are commonly used for matrix decomposition. These models extract different types of basis vectors according to predefined criteria and allow the construction of relevant lower-dimensional features by projection. These approaches for tracking the dynamic nature of FC generally assume that the timing of the various states is predetermined, that at each time point the brain is in a discrete state, or that the current state is a weighted sum of FC-states.<sup>[7,8,10]</sup> Although these assumptions may be valid for resting-state FC studies, task-based research presume that FC states remain quasi-stationary over time.<sup>[11-13]</sup>

Hence, it is not sufficient to depend on one criterion, such as ICA or PCA, to capture all essential components of brain connectivity. Singular value decomposition (SVD) has severe shortcomings when treating multidimensional data such as EEG recordings, because correlations stretch over more than one dimension,<sup>[14,15]</sup> but cannot manage the data segments of different lengths, an issue that often arises in brain analysis.<sup>[15]</sup> As a result, a key expansion to present methodologies would be to include algorithms for detecting time points when large changes in network organization occur. Given that multiple constraints, such as nonnegativity, sparsity, smoothness, or orthogonality, can be imposed on the factor matrices in various modes, it is important to recognize that statistical independence like in ICA and PCA is not the sole approach for extracting brain sources or isolating brain networks.

Therefore, it is necessary to study the brain connections with a comprehensive approach using EEG data using method that capability of compromising hidden variables and the high dimension of data in time. Combining techniques with various criteria and decomposing algorithms are indispensable to accurately preserve all the necessary components. Multiway data analysis extends beyond common linear methodologies to identify multilinear patterns and underlying relationships in higher-order datasets, often referred to as tensors.

Multiway data analysis extends linear methods to capture multilinear patterns and underlying relationships

within higher-order datasets, commonly referred to as tensors. Various tensor decomposition techniques have been developed for this purpose, including Canonical Decomposition also known as parallel factor analysis (PARAFAC) and Tucker decomposition.<sup>[16-19]</sup>

Tensor analysis, extends linear methods to capture multilinear patterns within high-order datasets, enabling a deeper understanding of complex relationships.<sup>[16-19]</sup> With flexibility for imposing constraints such as nonnegativity or sparsity, Tucker decomposition supports diverse applications, especially in brain network analysis via EEG.<sup>[17,19-21]</sup> Recent advances now enable the detection of significant change points in network connectivity, aiding in summarizing FCNs across the intervals of cognitive relevance.<sup>[17,20,21]</sup> In the context of tensor analysis, subspaces can often represent the certain properties or features of tensors (e.g., span of eigenvectors or principal components). It is necessary to compare the differences between the subspaces or states. As one of the most commonly used methods for this purpose, the Grassmann distance provides a way to measure how different two such subspaces are.

Our proposed study addresses the problem by keeping the network structure of FCNs intact by using tensor representations to identify the dynamic changes in time where significant changes to the network structure occur across all subjects due to interventions.

In this study, we aimed to investigate the brain dynamic connectivity changing points using analysis of Tucker decomposition method to identify FC matrices and summarize network structures. Through tensor representation, we can capture the variability which is common to all subjects across time using the analysis of variance (ANOVA). We hypothesized that A relatively similar network structure exists for all subjects. Once the change points are detected, the network state for the time intervals among change points is assumed to be stationary and common across subjects, and summarized through tensor-matrix projections across subjects, frequency and time. Brain activity in source domain obtained from high-density EEG data from 30 tinnitus patients was used in three different types of visual-only stimulation intended to induce pleasant sensations, visual combined with high-definition transcranial direct current stimulation (HD-tDCS), and visual combined with sham stimulation. Tinnitus is often associated with altered activity in auditory, somatosensory, and limbic systems.<sup>[22]</sup> Limiting stimulation paradigms to visual stimuli might fail to engage the auditory cortex or the neural networks most directly implicated in tinnitus perception and modulation. Visual stimuli are not directly related to the subjective auditory experience of tinnitus. Using only visual inputs may fail to simulate real-world conditions where auditory and somatosensory systems play significant roles in perception and modulation. Functional

targeting hypothesizes that the visual with tDCS targeting effect is contingent by modulating persistent function.

## Materials and Methods

### Participants

In this study, we used the data from 30 patients (18 male,  $54.43 \pm 10.31$  years) referred to the Centro Especializado de Otorrinolaringologia e Fonoaudiologia at the Clinical Hospital of Ribeirao Preto, Medical School-University of Sao Paulo (HCRP) in Brazil (HCRP No. 55716616.1.1001.5440).<sup>[22]</sup> Patients with consistent bilateral subjective tinnitus, auditory thresholds ranging from normal hearing to severe sensorineural hearing loss, no history of psychoactive drugs, normal color vision, and literacy/education are eligible. The study excludes patients with pulsatile tinnitus, Meniere illness, otosclerosis, chronic headaches, and neurological problems such as brain tumors, as well as those receiving mental health treatment. All the recruited participants underwent pure-tone audiometry (125–16,000 Hz) for hearing assessment at recruiting time. Psychoacoustic evaluation of tinnitus was performed at recruiting time and before and after each session.

### Experimental design

The protocol and data structure are completely explained in the study of Ghodratiostani *et al.*<sup>[22]</sup> A brief summary of the data acquisition and protocol is provided below:

Data were acquired in an observational crossover-sectional, randomized, and single-blind study across three sessions: (1) picture presentation visual stimulation (presenting a set of validated emotionally laden pictures for induction of positive emotions./positively emotionally charged pictures/positive pictures high positively valenced pictures from the Nencki Affective Picture System<sup>[22]</sup>); (2) visual stimulation picture presentation with HD-tDCS (20 min) (3) Visual stimulation picture presentation with sham. In the Sham procedure, only a small amount of current is applied to maintain the sensation of actual stimulation [Figure 1].

In the experiment, visual stimuli consisting of neutral and positive pictures were presented at a fixed screen location with a resolution of  $1600 \times 1200$  pixels. Neutral pictures are selected with the valence rate of higher than 4 and lower than 6 and the arousal rate lower than 6. A set of 20 neutral pictures in four loops is presented in the same order per loop. The order of presentation is randomized per session. Each picture is presented for 5 s with a cue of 500 ms in between. Neutral pictures are placed in the resting-state block (duration = 2 min) that starts and finishes with tinnitus loudness question “Scale your tinnitus loudness from 1 to 10.” Positive pictures are placed in the visual stimulation blocks, categorized into two different groups. The first group (HAV) contains four pictures with high arousal and high valence rated more than 6. The second

group (HV) contains 16 different pictures in each block with valence rate higher than 6.

During the experiment, eighty neutral pictures divided in four loops each containing twenty pictures, are presented to the patients. Two-hundred positive pictures are also displayed in five blocks with two loops; each block containing 20 pictures. The order of presentation for both neutral and positive pictures is the same. Each picture is presented for 5 s with a cue of 500 ms in between. The total time duration of picture presentation is almost 28 min. Throughout picture presentation, we frequently ask the patients to scale their tinnitus loudness from 1 to 10. In order to keep the patient’s conscious to their tinnitus perception.

Figure 2 shows that timeline of each three sessions is illustrated. The session with positive pictures without electrical stimulation is entitled Visual Stimulation in this schematic protocol. Visual stimulation is the session that we only have picture presentation without electrical stimulation. Each neutral picture group is presented for 2 min. The positive-valenced pictures presentation starts with presenting a fixed picture for 30 s during ramp up. (The fixed picture is presented for 30 s during ramp up.). While 30 s ramp down is included/merged in 20 min presentation of positive-valenced pictures.

High-density EEG (256 channels) is used to measure the changes in brain activity before, during, and after the tDCS. The EEG signal was recorded for 45 min per session. The 10 – 10 EEG Montage was used with a reference on Vertex (Cz) and recorded 1000 samples per second.

## Methods

### Preprocessing

For preprocessing, EEG data were initially labeled according to the timing of image presentations and different events. After labeling, the signal was segmented based on the timing of each event. First a bandpass filter (0.9–110 Hz) applied to EEG data to remove DC and keeping high-frequency information of the data.<sup>[23]</sup> Furthermore, a notch filter used to remove power line harmonics (50, 60, 100, and 120 Hz). Once the background noise caused by tDC stimulations is removed, then the signals were re-referenced to common average of electrodes and bad channels (channels with abnormally high amplitudes for extended periods, such as 5–20 s) were excluded. Bad segment rejection was applied to time segments where multiple electrodes (e.g., more than 10 electrodes) were saturated for durations exceeding 500 ms due to leaking gel among EEG electrodes and tDCS electrodes.<sup>[23,24]</sup> The bad segments were removed, and the missing data were reconstructed using interpolation by averaging the data before and after the removed segment to maintain temporal consistency for subsequent analyses. Following this, ICA was used to remove unwanted components such as nonbrain

activities, eye blinks, muscle activity, head movements, heartbeat artifacts, and other nonbrain components from the raw data by checking temporal activity and spectrum of the components using EEGLAB toolbox. Figure 3 shows preprocessing steps of EEG data in brief.

### Functional connectivity

The connectivity analysis of EEG plays a pivotal role in studying the brain's functional and structural networks, offering a window into the dynamic interactions between the neural regions. By quantifying how different areas of the brain communicate during various tasks, connectivity measures help unravel the complex, networked organization of the brain. Focusing on source space EEG offers significant advantages. EEG recorded at the scalp mixes signals from multiple sources due to the volume conduction effect. Source localization separates these contributions, offering a clearer view of neural activity. Sensor space connectivity measures can be confounded by spatial leakage, leading to spurious connections and it localizes the activity to specific brain regions, providing more precise insights compared to scalp-level signals.<sup>[22]</sup>

Choosing the appropriate method that can mitigate the effects of volume conduction is critical for obtaining

reliable source localization results is important.<sup>[25,26]</sup> Volume conduction refers to the distortion of electrical brain signals as they traverse various tissues, including the skull and scalp, before reaching the EEG electrodes. This phenomenon complicates source localization because the recorded signals may not precisely reflect the actual brain activity. The electrodes capture a mixture of signals from multiple regions, making it difficult to pinpoint their true origin.

In this study low resolution electromagnetic tomography was used for EEG source localization because it allows for the reconstruction of brain activity patterns from the EEG data with relatively low noise and good spatial resolution. It utilizes the principle of minimizing the estimated error across various electrical activities, making it effective in localizing brain sources even when there are multiple sources present.<sup>[26,27]</sup>

Since the number of sources obtained in each brain region can vary and may differ across different events, our aim is to identify a single source to represent each brain region. Given that the signal with the highest power typically contains the most meaningful information, sources with the highest power were selected among the potential

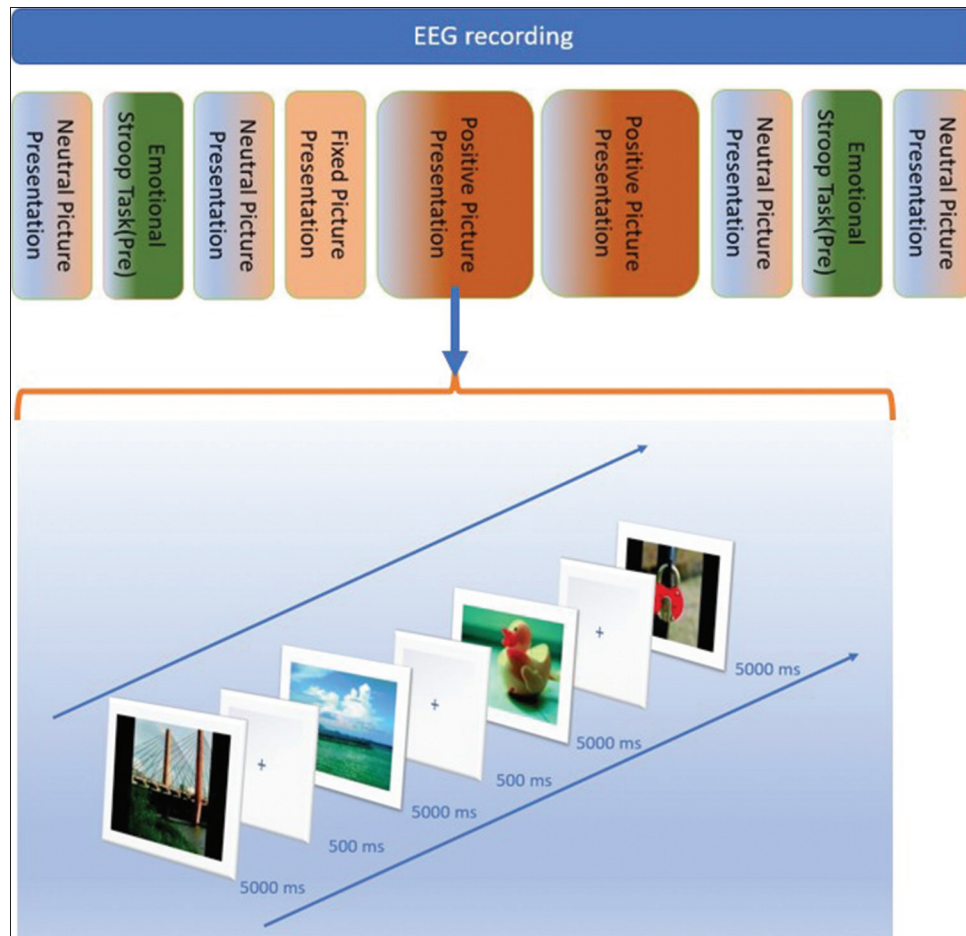


Figure 1: The sequence of picture presentation. EEG: Electroencephalogram

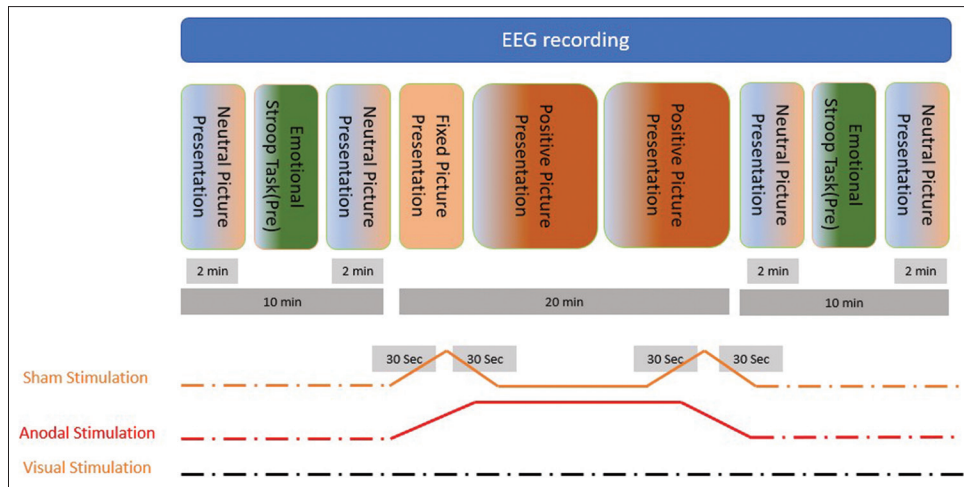


Figure 2: Time line of electrical stimulation. EEG: Electroencephalogram

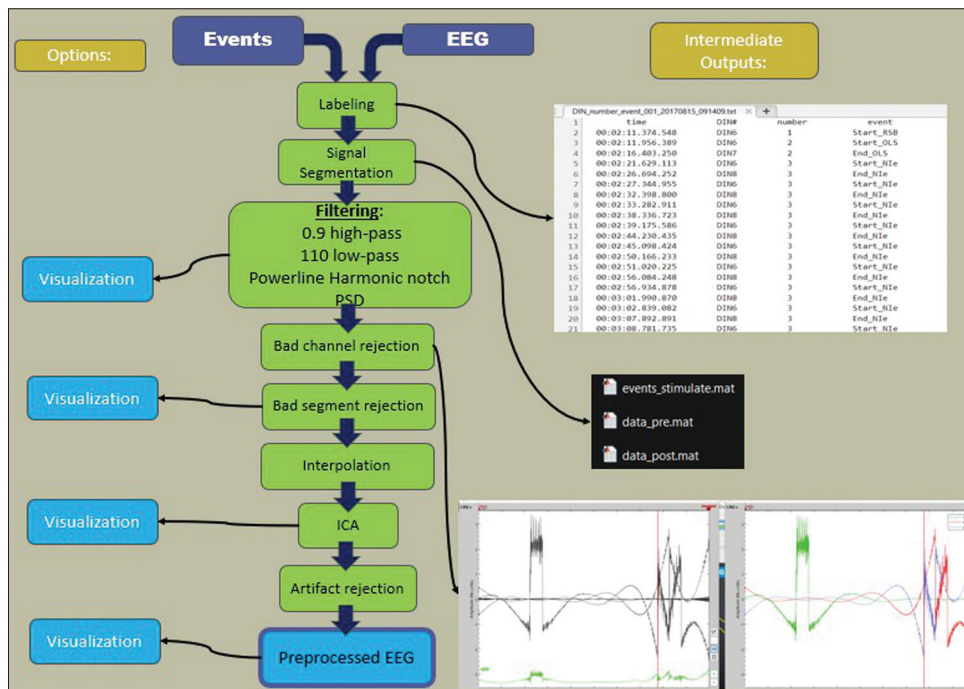


Figure 3: Preprocessing steps of electroencephalogram data. EEG: Electroencephalogram

sources within each brain region as the representative source.

The goal at this stage is to identify the change points in the FC matrix of selected sources using tensor decomposition methods.

After obtaining potential sources for each brain region the FC matrix computed for these sources using the phase locking value (PLV) method.<sup>[28]</sup> PLV is a widely used measure to evaluate phase synchronization between two signals, indicating the consistency of phase differences over time.<sup>[28-30]</sup> PLV is defined as:

$$PLV = \left| \frac{1}{N} \sum_{j=1}^N e^{i(\phi_{1(t)} - \phi_{2(t)})} \right| \quad (1)$$

Where  $\phi_{1(t)}$  and  $\phi_{2(t)}$  are the instantaneous phases of the two signals at time  $t$ , and  $N$  is the number of time points.

For each session connectivity matrices of 14 selected sources, with the dimensions of the matrices being  $256 \times 256$ , representing the pairwise FC among the 256 EEG channels. For each session of data recording, ultimately  $E$  FC matrices were obtained. Using these matrices, a tensor with dimensions  $S \times S \times E$  was created, where  $S$  represents the number of selected sources with high power and  $E$  represents the number of events that occurred during the experiment.

Here in our study, we also needed to capture the effect of the stimuluses also in different frequency bands of EEG. For group analysis, all FC matrices were included from

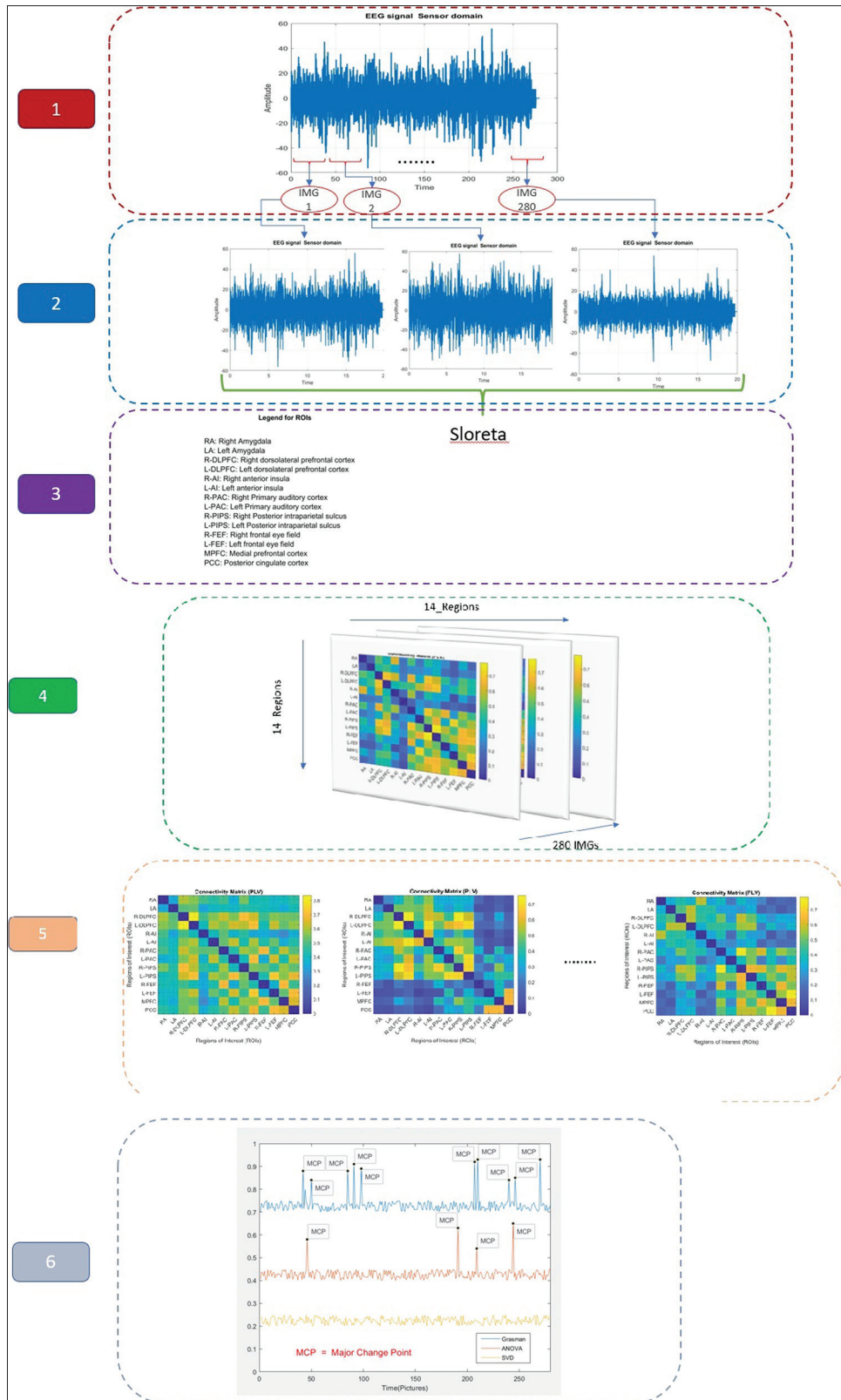
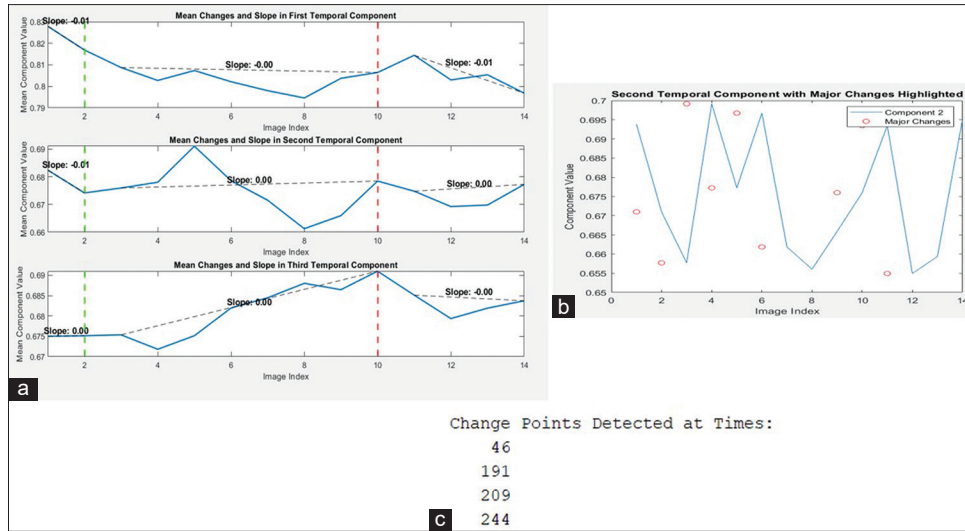


Figure 4: Diagram of approach for tensor decomposition of connectivity matrices of electroencephalogram sources to identify the dynamic change points. EEG: Electroencephalogram

different patients as an additional dimension in the tensor, resulting in a tensor with dimensions  $S \times S \times E \times N$ ,

where  $S$  represents the potential sources,  $E$  the events that occurred, and  $N$  the number of patients.



**Figure 5:** Estimated changing points out of applying the analysis of variance-based approach a) Mean change points and slope of change. b) Second temporal component with the major changes. c) Actual change points detected in time

As explained, in the context of tinnitus research, brain data involves multiple dimensions, such as EEG signals over time, different brain regions, and various frequency bands. Tensors processing allow us to capture and analyze this multidimensional structure in its entirety, preserving the relationships among these dimensions.

### Tensor decomposition

Blind source separation (BSS) is a signal processing technique that involves recovering unobserved source signals from a mixture of observed signals.<sup>[31]</sup> Tensor decomposition is a powerful tool for BSS as it effectively manages multidimensional data, such as time, place, and frequency, common in brain connectivity studies. Unlike traditional matrix-based methods, tensor approaches preserve natural multidimensional relationships, enabling more accurate extraction of hidden components like brain signals. This is crucial for isolating and identifying brain connectivity patterns associated with tinnitus, providing insights into neural processes and connectivity changes. Constraints like sparsity or nonnegativity are often applied to ensure the results are relevant and interpretable, aiding in the discovery of meaningful components. In some cases, the data matrix is divided into three or more parts to enhance the analysis. In the specific case of SVD of the data Matrix  $\mathbf{Y} \in \mathbb{R}^{I \times T}$ , the following factorization is applied:

$$\mathbf{Y} = \mathbf{A}\mathbf{D}\mathbf{B}^T = \mathbf{D} \times_1 \mathbf{A} \times_2 \mathbf{B} = \sum_j d_{jj} \mathbf{a}_j \mathbf{b}_j^T \quad (2)$$

Where  $\mathbf{A} \in \mathbb{R}^{T \times T}$  and  $\mathbf{B} \in \mathbb{R}^{T \times T}$  are orthogonal matrices and  $\mathbf{D}$  is a diagonal matrix containing only nonnegative singular values. The SVD and its generalizations play key roles in signal processing and data analysis.<sup>[31,32]</sup>

Multiple subjects, multiple task data sets can be represented by a set of data matrices  $\mathbf{Y}_n$  and it is necessary to perform simultaneous constrained matrix factorizations.

$$\mathbf{Y}_n \cong \mathbf{A}_n \mathbf{B}_n^T \quad (n = 1, 2, \dots, N) \quad (3)$$

Tucker model is especially effective for multiway BSS, feature extraction, and classification because it collects spatial, temporal, and spectral information and connects derived components to meaningful physiological interpretations.<sup>[17,32]</sup> Tucker decomposition reduces the dimensionality of the data by breaking it into a core tensor and factor matrices.<sup>[31,32]</sup> The core tensor captures the essential interactions among dimensions, while the factor matrices represent patterns in individual modes (e.g., spatial or temporal). This reduces computational complexity and noise while retaining key signal features. Also, Tucker decomposition can isolate noise components and focus on the true underlying patterns, aiding in artifact removal and signal enhancement.<sup>[28-31]</sup> The method is increasingly used in data fusion, dimensionality reduction, and pattern identification, making it ideal for complicated neuroimaging data processing.<sup>[17,32-36]</sup>

In the case of multidimensional data, the simple linear BSS model can be straightforwardly extended to multiway BSS models using constrained tensor decompositions. A general and flexible approach considered here takes advantage of the Tucker decomposition model shown in Eq. 4 which is also referred to as the Tucker-N model:<sup>[17]</sup>

$$\begin{aligned} \underline{\mathbf{Y}} &= \sum_{j_1=1}^{J_1} \sum_{j_2=1}^{J_2} \dots \sum_{j_N=1}^{J_N} \mathbf{g}_{j_1 j_2 \dots j_N} \left( u_{j_1}^{(1)} \circ u_{j_2}^{(2)} \circ \dots \circ u_{j_N}^{(N)} \right) + \underline{\mathbf{E}} \\ &= \underline{\mathbf{G}} \times_1 \mathbf{U}^{(1)} \times_2 \mathbf{U}^{(2)} \dots \times_N \mathbf{U}^{(N)} + \underline{\mathbf{E}} = \underline{\mathbf{G}} \times \{ \mathbf{U} \} + \underline{\mathbf{E}} = \hat{\underline{\mathbf{Y}}} + \underline{\mathbf{E}} \end{aligned} \quad (4)$$

Where  $\underline{\mathbf{Y}} \in \mathbb{R}^{I_1 \times I_2 \times \dots \times I_N}$  is the given data tensor,  $\underline{\mathbf{G}} \in \mathbb{R}^{J_1 \times J_2 \times \dots \times J_N}$  is a core tensor of reduced dimension,  $\mathbf{U}^{(1)} = [\mathbf{u}_1^{(1)}, \mathbf{u}_2^{(1)}, \dots, \mathbf{u}_{j_1}^{(1)}] \in \mathbb{R}^{I_1 \times J_1}$  ( $n = 1, 2, \dots, N$ ) are factors (component matrices) representing components, latent variables,

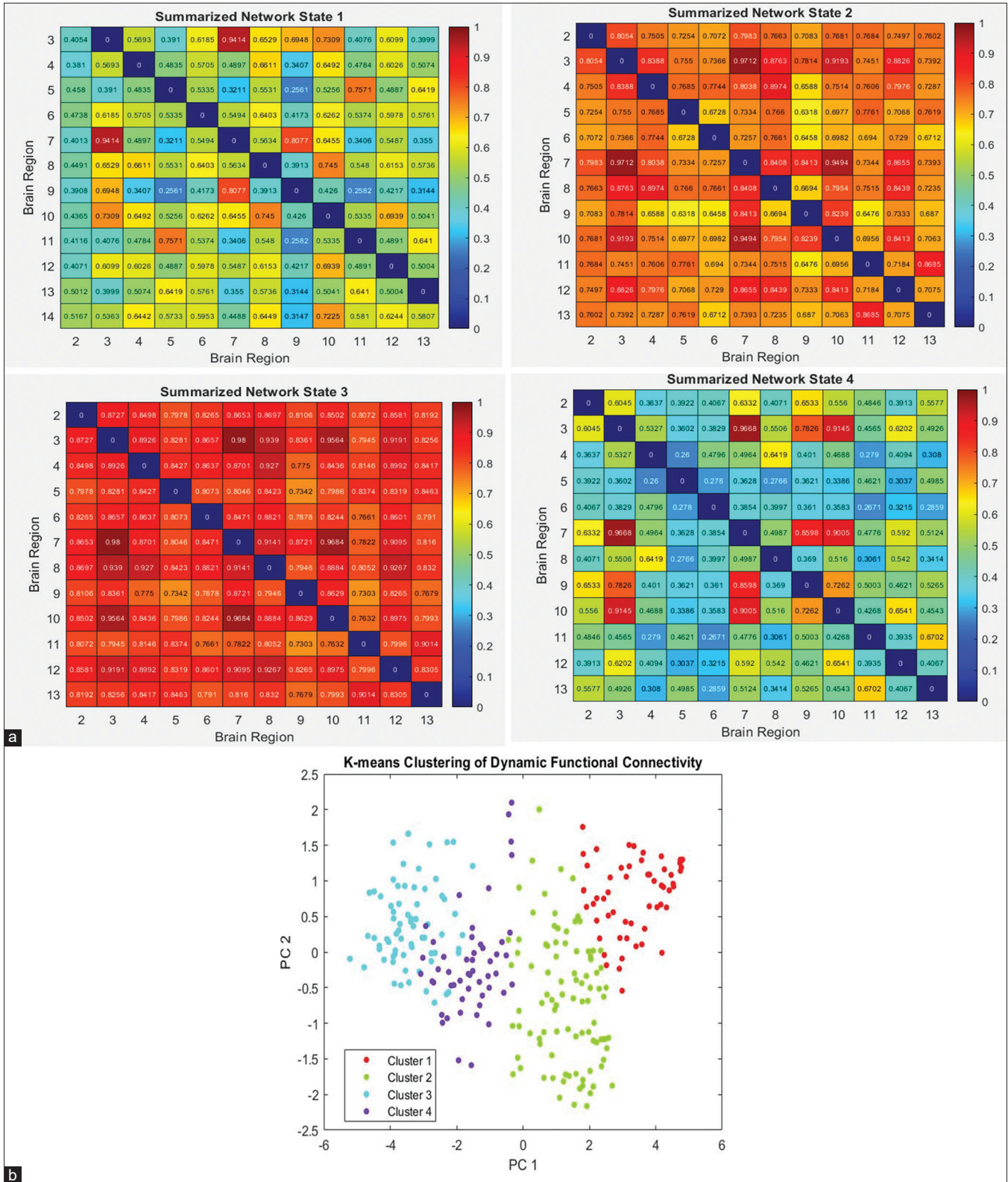


Figure 6: (a) connectivity matrices among the major change points, (b) Clustering Connectivity Matrices Using K-mean

common factors or loadings,  $Y$  is an approximation of the measurement  $Y$ , and  $E$  denotes the approximation error or noise depending on the context. The objective is to estimate factor matrices:  $U^{(n)}$ , with components (vectors)

$u_{j_n}^{(n)}, (n=1,2,\dots,N, j_n=1,2,\dots,J_n)$  and the core tensor  $G \in \mathbb{R}^{J_1 \times J_2 \times \dots \times J_N}$  assuming that the number of factors in each mode  $J_n$  are known or can be estimated.<sup>[35-37]</sup>

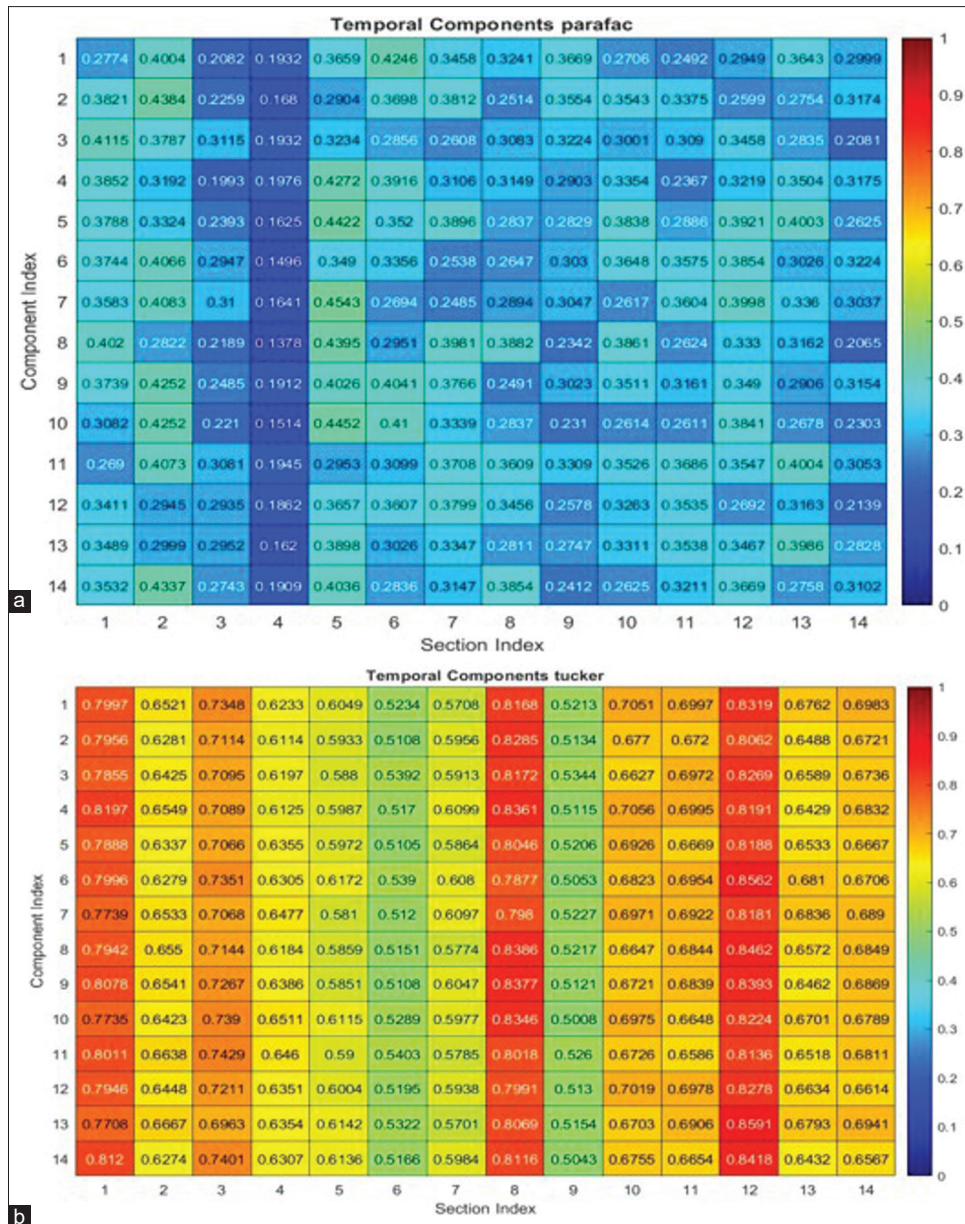


Figure 7: (a) Temporal components variation by parallel factor analysis decomposition, (b) Temporal components variation by TUCKER decomposition

Since we aimed to identify the major change points, this study combined Tucker with ANOVA<sup>[38]</sup> to capture the dynamic variations and first-order derivative and Grossman,<sup>[39]</sup> as follows:

- In the ANOVA based method, the slope of the tangent line was calculated, and based on the changes in the slope, the change points were identified
- In the first-order derivative method, change points were identified based on 95% threshold of derivative changes in the connectivity matrix that corresponds to the significance level.<sup>[18]</sup>

While the Tucker decomposition cannot determine the component matrices uniquely like PARAFAC, its component matrices are orthogonal. The orthogonality property of the

Tucker decomposition makes it an appropriate decomposition for lower dimensional subspace projection and the core array.<sup>[18,36,37]</sup> As the Tucker decomposition is a higher-order generalization of SVD for tensors, first elements are the most important singular values which enables us low approximation. Hence, based on connectivity matrices, we made the tensor including different modes, then using Tucker as explained we got the most important singular information and investigated variations using the ANOVA [Figure 4].

Once the major changes were identified, new FC matrices were computed among these points. Finally, K-means was employed to compare the FC matrices among major change points as it has been employed in several EEG connectivity studies.<sup>[18,37,40]</sup> This clustering approach allowed us to quantitatively evaluate the significant differences in the

FC matrices at various time intervals, providing deeper insights into how brain networks evolved across different experimental phases.

As shown in Table 1, the regions involved in tinnitus are displayed. In addition, Figure 4 presents the flowchart for obtaining the signal corresponding to each time segment., The representative time signals for each region during the prestimulation, stimulation, and poststimulation phases are provided in Figure 4.

Results of analysis based on the explained method on which decomposition method showed better results and

results related to ANOVA to reveal the changing points of connectivity report in the following.

**Experimental results**

Based on the results, we proceeded with the Tucker decomposition method for further analysis. Here, we wanted to know which images as visual stimulus caused significant change in dynamic connectivity. Totally, EEG data are divided into 14 segments: the first two-time sections corresponded to the prestimulus phase, the next 10 segments corresponded to the stimulation phase, and

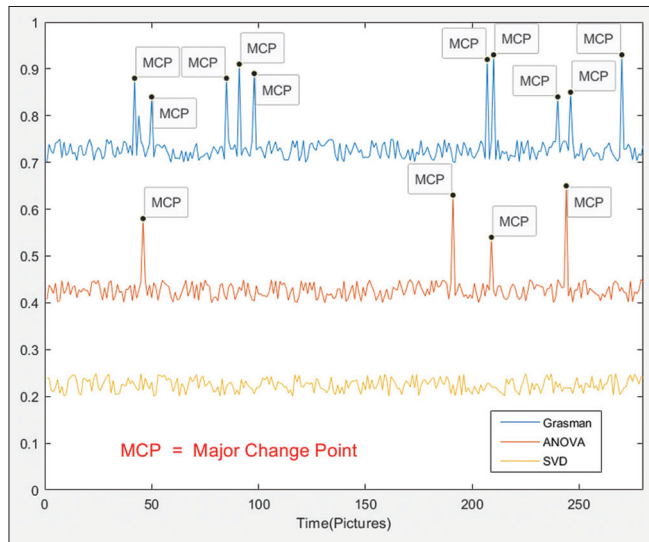


**Figure 8: Most significant change points among the consecutive time steps of the functional connectivity network calculated based on singular value decomposition and tensor projection**

**Table 1: Regions involved in tinnitus**

Network	Seeds	MNI coordinates		
		X	Y	Z
Emotion processing	Right amygdala	18	-7	-17
	Left amygdala	-17	-2	-24
FPN	Right dorsolateral prefrontal cortex	41	38	30
	Left dorsolateral prefrontal cortex	-43	33	28
CON	Right anterior insula	47	14	0
	Left anterior insula	-44	13	1
AN	Right primary auditory cortex	41	-27	6
	Left primary auditory cortex	-55	-22	9
DAN_1	Right posterior intraparietal sulcus	26	-62	53
	Left posterior intraparietal sulcus	-23	-70	46
DAN_2	Right frontal eye field	27	-11	54
	Left frontal eye field	-25	-11	54
DMN	Medial prefrontal cortex	8	59	19
	Posterior cingulate cortex	-2	-50	25

DMN – Default mode network; AN – Auditory network; CON – Cingulo-opercular network; FPN – Fronto-parietal network; DAN – Dorsal attention network; MNI – Montreal neurological institute

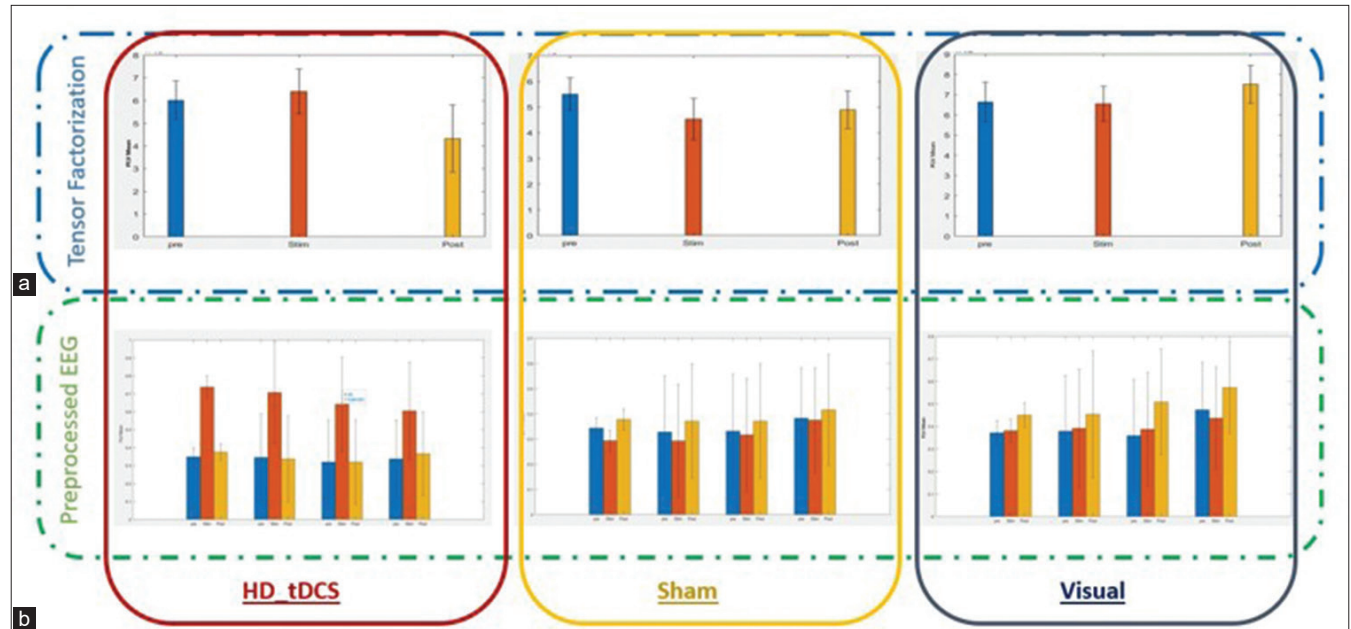


**Figure 9: Bar chart of the mean and standard error of phase locking value values before, during, and after stimulation for visual positive emotion induction combined with high-definition-transcranial direct current stimulation and Sham sessions using the tensor decomposition method. a) Mean PLV with tensor factorization (Upper row). b) Mean PLV without tensor factorization. HD-tDCS: High-definition transcranial direct current stimulation**

the final 2 segments corresponded to the poststimulus phase.

### *Tucker-analysis of variance*

We used the ANOVA slope method to identify the major change points of each region among detected time sections by Tucker (sections 1, 8 and 12). First, ANOVA was computed for connectivity changes in detected segments of specified region, and then the slope of changes tracked using the following method: the slope was calculated for each time section relative to the previous segment, and any point where the slope exceeded 90% of the total slope changes was considered a major change point.

As shown in Figure 5a, the method using the slope tangent to the ANOVA successfully revealed major change points. Figure 6b, which illustrates these change points, shows that the first change point occurs at image number 46. Given that the patient was shown 40 images prior to stimulation (arranged in two loops of 20 images each) and 200 images during stimulation with the tDCS device activated during the first loop of the stimulation phase, the algorithm has accurately detected the change point, which appears in the initial loop following the onset of stimulation. The second change point occurs at image number 209, which may result from the continued effect of tDCS stimulation. The final change point occurs at image number 244, which coincides with the time when the tDCS device was turned off, causing a major change in the brain's FC. As shown in Figure 5c, exact time of major change point in connectivity are detected by method.

After identifying the major change point, as shown in Figure 6a, the connectivity matrices were calculated among the major change points, with the results for the visual with HD-tDCS session. In the next step, to quantify the changes in the obtained connectivity matrices, we converted the connectivity matrices into vectors and clustered the resulting vectors using the K-means method. As shown in Figure 6b, the mean of each cluster, corresponding to the connectivity matrix among the major change points (significant sections of time detected by Tucker), differed from one another. As a result, the obtained connectivity matrices can be considered the main connectivity matrices at each stage.

### *Method validation*

As shown in Figure 7a, we can see PARAFAC decomposition did not effectively detect connectivity changes in time mode (the connectivity changes over the 14-time sections for mean all 280 images shown to patient did not show significant differences). However, as shown in Figure 7b, the changes in connectivity were successfully identified using the Tucker decomposition (the most significant changes were observed in time sections 1, 8, and 12, which correspond to the prestimulation, stimulation,

**Table 2: Silhouette score of change points detected from Tucker-analysis of variance and Tucker-Grassman**

Change points	Silhouette score	
	Tucker-ANOVA	Tucker-Grassman
1-2	0.4	0.3
1-3	0.6	0.5
1-4	0.7	0.6
2-3	0.6	0.4
2-4	0.7	0.5
4-3	0.4	0.3
Mean	0.56	0.43

ANOVA – Analysis of variance

and poststimulation phases, respectively).

Based on Table 2, dispersion of samples in clusters related together that means how points in a cluster (time section of stimuli) are far from another one using Silhouette score. As we can see, points in clusters are good clustered using k-mean by Tucker-ANOVA which means PLV values of major change points are significantly differ from each other.

In order to show the effectiveness of tensor-based methods compared to the traditional matrix-based methods, the upper triangle part of connectivity matrix which was vectorized and concatenated across subjects to form a matrix to perform tensor decomposition. Similarly, SVD is performed on the matrices at each time step similar to the tensor approach without subject sampling. An optimal rank at each time point is determined using the convex hull algorithm. Given the rank at each time, the Grassmann distance among consecutive time steps is computed concatenated across subjects to form a matrix. As we can see in Figure 8, SVD couldn't find any significant change points comparing the two other methods based on tensor decomposition. Results also showed that Tucker-ANOVA could outperform Grassman because of the sparser results of our approach.

## **Discussion**

In this study, our aim was to investigate the effects of stimulation on changing dynamic of brain connectivity positive emotion induction (PEI) by visual and brain stimulations. For this, the high-density EEG data of tinnitus patients were used to investigate dynamic changes in brain connectivity under different states of stimulation types of visual Positive Emotion Induction (PEI) stimulation, PEI with HD-tDCS, and PEI combined with sham stimulation. Connectivity of data in source domain was calculated then using tensor decomposition methods which is capable of handling high-dimensional data, we tried to investigate change points if dynamic connectivity based of variation in results of time domain of results of decompositions methods.

First of all, based on our results, Tucker method showed promising results of decomposition of the high dimensional

connectivity matrices (including modes as time domain, frequency and subjects). Our results did not show significant changes using PARAFAC [Figure 5a and b]. Tucker decomposition allows for a more flexible core tensor with fewer constraints, which enables it to capture more complex interactions among tensor modes. PARAFAC imposes a stricter structure on the data, with the factor matrices constrained to vary only along one mode while being identical across others, which can limit its ability to capture complex patterns and our results are along with this that Tucker method revealed us significant sections of stimuli which connectivity varied related to other sections. Our results are aligning with previous researches on effectiveness of Tucker to conventional ones when dealing with neural data.<sup>[17,18,37,40]</sup>

Based on that connectivity of the detected section were calculated. Figure 8 presents the average connectivity matrices before, during, and after stimulation. The top row shows the average connectivity using the tensor decomposition method, while the bottom row displays the average connectivity with preprocessed data using the PLV method for four frequency bands of alpha, beta, delta, and theta.

As shown in Figure 9, for the PEI combined with HD-tDCS session (left column), the average connectivity during stimulation has the highest value, both with and without tensor decomposition. On the other hand, in the method without tensor decomposition, the average connectivity values before and after stimulation are almost similar. However, with tensor decomposition, the average connectivity before and after stimulation shows a notable difference, with poststimulation connectivity being lower than prestimulation. This suggests that tensor decomposition can effectively differentiate meaningful connectivity.

In the Sham session (middle column), the average connectivity is almost the same across all segments in both methods. However, the noteworthy point here is the pattern of the connectivity averages, where the matrix's average connectivity is the highest before stimulation and lowest during stimulation. This pattern is well-preserved when using the tensor decomposition method. In the visual session (right column), similar to the Sham session, the changes in the average connectivity matrices are not significant. However, the pattern of changes in the average connectivity matrices using the tensor decomposition method is still preserved in this session as well.

Based on Table 2, we can see clustering PLV of detected change points [sections 1, 3, 8, and 12, as shown in Figure 5] by Tucker are successfully differ from each other. This is aligned with Figure 9 which we seen that mean PLV of sections in prestimuli, stimuli and poststimuli are different significantly. Hence, Tucker detected section as change points correctly.

However, an important point is that stimulation using PEI along with tDCS caused significant increase in PLV in all frequency range off EEG comparing to sham and only visual stimulation but as it can be seen in Figure 9a, the standard deviation before applying tensor decomposition is significantly higher compared to after applying tensor decomposition, indicating that tensor decomposition can effectively extract important and meaningful connectivity [Figure 9b].

Recent studies have utilized Tucker tensor decomposition to analyze EEG data, revealing dynamic brain states based on multiway tensors reconstructed from time, frequency, regions or subjects.<sup>[18,37,40-45]</sup> These studies highlight the efficacy of Tucker decomposition in decoding complex, multidimensional EEG data as our results acknowledged efficiency of Tucker. Although Tucke has been widely used in similar studies, it is important to provide a criterion for identifying change points based on Tucker's results. Mahyari *et al.*, proposed the Grossman to identify change points in time<sup>[18]</sup> but in this study, we used a criterion based on variations in Tucker's component values, which was not only better than Grossman and SVD, but also provided more sparser results, as shown in Figure 8.

The results showed that in patients with tinnitus, visual stimulation alone – intended to induce pleasant sensations – may fail to yield the significant changes in the connectivity networks. Tinnitus is often associated with altered activity in auditory, somatosensory, and limbic systems.<sup>[46,47]</sup> Limiting stimulation paradigms to visual stimuli might fail to engage the auditory cortex or the neural networks most directly implicated in tinnitus perception and modulation. Visual stimuli are not directly related to the subjective auditory experience of tinnitus. Using only visual inputs may fail to simulate real-world conditions where auditory and somatosensory systems play significant roles in perception and modulation. Patients with tinnitus show variability in how visual and auditory stimuli influence their neural processing. Visual-only paradigms may not address this heterogeneity, limiting the generalizability of results to the broader tinnitus population. Our results are consistent with the need to use tDCS along with visual stimuli for more effective intervention in tinnitus patients.

As future work, we suggest using EEG-fMRI signals to gain more insight into functional networks in tinnitus and allow for better detection of connectivity changes associated with the disorder and treatments.

## Conclusion

The major change points identification and summarization of FCNs in both source spaces were performed using the tensor decomposition method presented in this paper. Moreover, by applying tensor decomposition in the source space, we could identify with high accuracy the major changes in the connectivity matrices through Tucker-

ANOVA based approach. Most importantly, Upon the achieved results we suggested that in patients with tinnitus, visual stimulation alone—intended to induce pleasant sensations—may fail to yield significant changes in the connectivity networks. Due to promising results of Tucker-ANOVA for identifying major changing points in dynamic brain connectivity, it can be used in various fields related to the analysis of changes in brain connections in the presence of therapeutic interventions or based on performing cognitive activities.

### Financial support and sponsorship

This study is funded by Tehran University of medical Sciences with grant no. 1400-2-101-46982.

### Conflicts of interest

There are no conflicts of interest.

### References

1. Chu CJ, Tanaka N, Diaz J, Edlow BL, Wu O, Hämäläinen M, *et al.* EEG functional connectivity is partially predicted by underlying white matter connectivity. *Neuroimage* 2015;108:23-33.
2. Xie W, Toll RT, Nelson CA. EEG functional connectivity analysis in the source space. *Dev Cogn Neurosci* 2022;56:101119.
3. Allen EA, Damaraju E, Plis SM, Erhardt EB, Eichele T, Calhoun VD. Tracking whole-brain connectivity dynamics in the resting state. *Cereb Cortex* 2014;24:663-76.
4. Dimitriadis SI, Laskaris NA, Micheloyannis S. Transition dynamics of EEG-based network microstates during mental arithmetic and resting wakefulness reflects task-related modulations and developmental changes. *Cogn Neurodyn* 2015;9:371-87.
5. Dimitriadis SI, Laskaris NA, Tzelepi A. On the quantization of time-varying phase synchrony patterns into distinct functional connectivity microstates (FCstates) in a multi-trial visual ERP paradigm. *Brain Topogr* 2013;26:397-409.
6. Leonardi N, Richiardi J, Gschwind M, Simioni S, Annoni JM, Schluep M, *et al.* Principal components of functional connectivity: A new approach to study dynamic brain connectivity during rest. *Neuroimage* 2013;83:937-50.
7. Mehrkanoon S, Breakspear M, Boonstra TW. Low-dimensional dynamics of resting-state cortical activity. *Brain Topogr* 2014;27:338-52.
8. Mutlu AY, Bernat E, Aviyente S. A signal-processing-based approach to time-varying graph analysis for dynamic brain network identification. *Comput Math Methods Med* 2012;2012:451516.
9. Betzel RF, Erickson MA, Abell M, O'Donnell BF, Hetrick WP, Sporns O. Synchronization dynamics and evidence for a repertoire of network states in resting EEG. *Front Comput Neurosci* 2012;6:74.
10. Leonardi N, Shirer WR, Greicius MD, Van De Ville D. Disentangling dynamic networks: Separated and joint expressions of functional connectivity patterns in time. *Hum Brain Mapp* 2014;35:5984-95.
11. Lowe MJ, Beall EB, Sakaie KE, Koenig KA, Stone L, Marrie RA, *et al.* Resting state sensorimotor functional connectivity in multiple sclerosis inversely correlates with transcallosal motor pathway transverse diffusivity. *Hum Brain Mapp* 2008;29:818-27.
12. Jolliffe IT, Cadima J. Principal component analysis: a review and recent developments. *Philosophical transactions of the royal society A: Mathematical, Physical and Engineering Sciences*. 2016;374:20150202.
13. Comon P. Independent component analysis, a new concept? *Signal Process* 1994;36:287-314.
14. De Lathauwer L, De Moor B, Vandewalle J. On the best rank-1 and rank-( $r_1, r_2, \dots, r_n$ ) approximation of higher-order tensors. *SIAM J Matrix Anal Appl* 2000;21:1324-42.
15. Cichocki A, Zdunek R, Choi S, Plemmons R, Amari SI. Non-negative tensor factorization using alpha and beta divergences. In 2007 IEEE International Conference on Acoustics, Speech and Signal Processing-ICASSP'07. *EEE*; 2007;3:III-1393.
16. Kolda TG, Bader BW. Tensor decompositions and applications. *SIAM Rev* 2009;51:455-500.
17. Acar E, Yener B. Unsupervised multiway data analysis: A literature survey. *IEEE Trans Knowl Data Eng* 2008;21:6-20.
18. Mahyari AG, Zoltowski DM, Bernat EM, Aviyente S. A tensor decomposition-based approach for detecting dynamic network states from EEG. *IEEE Trans Biomed Eng* 2017;64:225-37.
19. Cong F, Lin QH, Kuang LD, Gong XF, Astikainen P, Ristaniemi T. Tensor decomposition of EEG signals: A brief review. *J Neurosci Methods* 2015;248:59-69.
20. Freyer F, Aquino K, Robinson PA, Ritter P, Breakspear M. Bistability and non-Gaussian fluctuations in spontaneous cortical activity. *J Neurosci* 2009;29:8512-24.
21. Chang C, Glover GH. Time-frequency dynamics of resting-state brain connectivity measured with fMRI. *Neuroimage* 2010;50:81-98.
22. Ghodratiostani I, Gonzatto OA Jr., Vaziri Z, Delbem AC, Makkiabadi B, Datta A, *et al.* Dose-response transcranial electrical stimulation study design: A well-controlled adaptive seamless Bayesian method to illuminate negative valence role in tinnitus perception. *Front Hum Neurosci* 2022;16:811550.
23. Al-Kaysi AM, Al-Ani A, Loo CK, Powell TY, Martin DM, Breakspear M, *et al.* Predicting tDCS treatment outcomes of patients with major depressive disorder using automated EEG classification. *J Affect Disord* 2017;208:597-603.
24. Dattola S, Morabito FC, Mammone N, La Foresta F. Findings about loreta applied to high-density EEG – A review. *Electronics* 2020;9:660.
25. Keeser D, Padberg F, Reisinger E, Pogarell O, Kirsch V, Palm U, *et al.* Prefrontal direct current stimulation modulates resting EEG and event-related potentials in healthy subjects: A standardized low resolution tomography (sLORETA) study. *Neuroimage* 2011;55:644-57.
26. Aydore S, Pantazis D, Leahy RM. A note on the phase locking value and its properties. *Neuroimage* 2013;74:231-44.
27. di Biase L, Ricci L, Caminiti ML, Pecoraro PM, Carbone SP, Di Lazzaro V. Quantitative high density EEG brain connectivity evaluation in Parkinson's disease: The phase locking value (PLV). *J Clin Med* 2023;12:1450.
28. Schmidt BT, Ghuman AS, Huppert TJ. Whole brain functional connectivity using phase locking measures of resting state magnetoencephalography. *Front Neurosci* 2014;8:141.
29. Cichocki A. Generalized component analysis and blind source separation methods for analyzing multichannel brain signals. *Statistical and Process Models for Cognitive Neuroscience and Aging* 2007;1:201-72.
30. Cichocki A. Blind signal processing methods for analyzing multichannel brain signals. *Int J Bioelectromagnetism* 2004;6:22-7.
31. Phan AH, Cichocki A. Tensor decompositions for feature extraction and classification of high dimensional datasets. *Nonlinear Theory Appl IEICE* 2010;1:37-68.
32. Weis M, Jannek D, Roemer F, Guenther T, Haardt M, Husar P.

- Multi-dimensional PARAFAC2 component analysis of multi-channel EEG data including temporal tracking. *Annu Int Conf IEEE Eng Med Biol Soc* 2010;2010:5375-8.
33. Makkiabadi B, Jarchi D, Sanei S. Blind Separation and Localization of Correlated P300 Subcomponents from Single Trial Recordings Using Extended PARAFAC2 Tensor Model. In: 2011 Annual International Conference of the IEEE Engineering in Medicine and Biology Society. IEEE; 2011.
  34. Naskovska K, Cheng Y, de Almeida AL, Haardt M. Efficient computation of the PARAFAC2 decomposition via generalized tensor contractions. In 2018 52<sup>nd</sup> Asilomar Conference on Signals, Systems, and Computers. IEEE; 2018. p. 323-7.
  35. Faghfour A, Shalchyan V, Toor HG, Amjad I, Niazi IK. A tensor decomposition scheme for EEG-based diagnosis of mild cognitive impairment. *Heliyon* 2024;10:e26365.
  36. Al-Sharoa E, Alwardat M, Aviyente S. Structured Robust Tensor Decomposition for Multilayer Community Detection: Application to Functional Connectivity Networks.
  37. Leonardi N, Van De Ville D. Identifying Network Correlates of Brain States Using Tensor Decompositions of Whole-Brain Dynamic Functional Connectivity. In: 2013 International Workshop on Pattern Recognition in Neuroimaging. IEEE; 2013.
  38. St Lars, Wold S. Analysis of variance (ANOVA). *Chemometr Intell Lab Syst* 1989;6:259-72.
  39. Nocera S, Zweifel P. The demand for health: An empirical test of the Grossman model using panel data. In: *Health, the Medical Profession, and Regulation*. Boston, MA: Springer US; 1998. p. 35-49.
  40. Karamzadeh N, Medvedev A, Azari A, Gandjbakhche A, Najafizadeh L. Capturing dynamic patterns of task-based functional connectivity with EEG. *Neuroimage* 2013;66:311-7.
  41. Abdi-Sargezeh B, Valentin A, Alarcon G, Martin-Lopez D, Sanei S. Higher-order tensor decomposition based scalp-to-intracranial EEG projection for detection of interictal epileptiform discharges. *J Neural Eng* 2021;18:066039.
  42. Mokhtari F, Laurienti PJ, Rejeski WJ, Ballard G. Dynamic functional magnetic resonance imaging connectivity tensor decomposition: A new approach to analyze and interpret dynamic brain connectivity. *Brain Connect* 2019;9:95-112.
  43. Rošáková Z, Rosipal R, Seifpour S. Tucker tensor decomposition of multi-session EEG data. In: *Artificial Neural Networks and Machine Learning-ICANN 2020: 29<sup>th</sup> International Conference on Artificial Neural Networks, Bratislava, Slovakia, Proceedings. Part I*. Springer International Publishing; 2020. p. 115-26.
  44. Seifpour S, Šatka A. Tensor decomposition analysis of longitudinal EEG signals reveals differential oscillatory dynamics in eyes-closed and eyes-open motor imagery BCI: A case report. *Brain Sci* 2023;13:1013.
  45. Mahyari AG, Aviyente S. Identification of Dynamic Functional Brain Network States through Tensor Decomposition. In: 2014 IEEE International Conference on Acoustics, Speech and Signal Processing (ICASSP). IEEE; 2014. p. 2099-103.
  46. Frusque G, Jung J, Borgnat P, Gonçalves P. Multiplex Network Inference with Sparse Tensor Decomposition for Functional Connectivity. *IEEE Trans Signal Inf Process Over Netw* 2020;6:316-28.
  47. Ghodratoostani I, Zana Y, Delbem AC, Sani SS, Ekhtiari H, Sanchez TG. Theoretical tinnitus framework: A neurofunctional model. *Front Neurosci* 2016;10:370.